Ventricular dilation as an instability of intracranial dynamics

R. Bouzerar,[1,*] K. Ambarki,[2] O. Balédent,[2] G. Kongolo,[3] J. C. Picot,[1] and M. E. Meyer[2]
[1]*Condensed Matter Physics Laboratory, UFR Sciences, Université de Picardie, 33 Rue Saint-Leu, 80039 Amiens, France*
[2]*Biophysics and Image processing Laboratory, CHU Nord Amiens, 3Pediatric unit, CHU Nord Amiens, France*
[3]*CHU Amiens Nord, Place Victor Pauchet, 80054 Amiens, France*
(Received 11 March 2005; published 8 November 2005)

We address the question of the ventricles' dilation as a possible instability of the intracranial dynamics. The ventricular system is shown to be governed by a dynamical equation derived from first principles. This general nonlinear scheme is linearized around a well-defined steady state which is mapped onto a pressure-volume model with an algebraic effective compliance depending on the ventricles' geometry, the ependyma's elasticity, and the cerebrospinal fluid (CSF) surface tension. Instabilities of different natures are then evidenced. A first type of structural instability results from the compelling effects of the CSF surface tension and the elastic properties of the ependyma. A second type of dynamical instability occurs for low enough values of the aqueduct's conductance. This last case is then shown to be accompanied by a spontaneous ventricle's dilation. A strong correlation with some active hydrocephalus is evidenced and discussed. The transfer function of the ventricles, compared to a low-pass filter, are calculated in both the stable and unstable regimes and appear to be very different.

DOI: 10.1103/PhysRevE.72.051912 PACS number(s): 87.19.Rr, 87.19.Xx, 87.10.+e, 87.80.Vt

I. INTRODUCTION

Apart from cognitive processes relying on neurobiological processes, the understanding of the intracranial machinery involves processes described by physical quantities. From Magendie [1] who in 1825 established that cerebrospinal fluid (CSF) moved by ebb and flow to the observation by O'Connel [2], around 1943, of the synchronization of CSF pulsations with cardiac pulses and its sensitivity to arterial and venous pressures changes, the relevance of physics was always attested. The characterization of these processes and their dynamics defines the field of the intracranial dynamics.

The intracranial dynamics is referred to as a set of biological, chemical and physical processes of different natures occurring inside the space demarcated by the rigid cranium. A natural hierarchy between these processes is established by their proper dynamics (though coupled between them) relying on different characteristic time scales. For instance, the dynamics of the cognitive processes is determined by neurons dynamics which is much more faster than the CSF flow monitored by the cardiac pulses, itself faster than the secretion or absorption process of CSF.

The building of an intuitive and predictive model of the intracranial dynamics is a challenging problem for both physicists and physicians. The attention of the physicist is focused on the obvious applicability of the physical laws to the intracranial processes, such as CSF and blood flow or brain matter elasticity. This venture is confronted with a serious difficulty, the complexity of the abovementioned system. This complexity reflects itself in many phenomena such as the structure of the system, its degree of organization and over all existence of (auto) regulation processes operating simultaneously. Achievement of such a purpose depends mainly on the reduction of that complexity, that is on the introduction of new concepts or theoretical methods allowing to bypass the difficulties associated with that complexity. A survey of the different attempts to circumvent these difficulties is given in the next section. These models might be classified mainly into two categories, ad hoc models such as electrical [3] and mechanical analogues [4] of the intracranial system and models derived from first principles. The most commonly encountered models belong to the first class to which a good critical review was devoted by Tenti *et al.* [5].

Whatever the physical modus operandi, the enterprise to be carried out profits by the great clinical advances of flow MRI [6]. Indeed, the development of this technique generated a great amount of knowledge of the CSF dynamics thanks to the recent introduction of phase-contrast magnetic resonance imaging (PCMRI) [7], which provides CSF and blood flow measurements throughout the cardiac cycle when used with peripheral cardiac gating. The attitude of the physician towards these observational data is of course dominated by clinical needs. But this does not prevent a more subtle understanding of the mechanisms underlying the intracranial processes. In our opinion, this purpose might be achieved only through an interpretation of observational data such as flow MRI, within the framework of (bio) physical model of the intracranial dynamics. The physical description of the mechanism underlying the intracranial processes is not the only virtue of a realistic and complete modeling which should also predict some abnormal behavior to be associated with some existing pathology. An example of these pathologies of the brain is hydrocephalus, trouble in keeping with the CSF flow [8]. This physiopathology of the brain consists in a ventricular enlargement. Many mechanisms for this trouble have been hypothesized by physicians [9]. Many models try to account for or describe the physiological ef-

*Corresponding author. Present address: Condensed Matter Physics Laboratory, UFR Sciences, Université de Picardie, 33 Rue Saint-Leu, 80039 Amiens, France. Email address: robert.bouzerar@sc.u-picardie.fr

 ©2005 The American Physical Society

fects of hydrocephalus with or without luck. It should be pointed out that the related models are always of the descriptive type (ad hoc models), that is do not contain this pathological behavior as a consequence. No further understanding of the disease is gained since these models also do not highlight the underlying mechanisms. Moreover, it is always difficult to extract order of magnitudes from the models to be compared to available medical data (and thus confirm or infirm some hypotheses) because of the lack of assessment of some parameters.

It is precisely in this ill-defined framework that we attempted to build up a model of the ventricular dynamics. In this work we focus on the ventricular compartment. Taking into account the elasticity of the ependyma as the fundamental element for regulating the ventricular volume, the CSF dynamical equations are derived and shown to belong to the PV models category but with an effective algebraic compressibility of CSF. The model is shown to exhibit a dynamical instability resulting in the intracranial pressure deregulation. A stability criterion involving only well defined parameters of the system (elastic properties of the ependyma, geometry of the ventricular area, compliance of CSF) is derived and its relation to hydrocephalus discussed.

II. SURVEY OF THE DIFFERENT TYPES OF MODELS

During the past three decades, a large number of mathematical models have been proposed to help physicians to better understand the complexity of the intracranial hydrodynamics. The reduction of the complexity of the brain-CSF system apart from the cognitive aspects might be realized in several ways. Before commenting on these different models, it should be noticed that there exists an irreducible anatomical ingredient common to all types of models: the intracranial system subdivision into well defined (and known) compartments. These compartments are the ventricular space filled with CSF, the parenchyma irrigated with the arterial blood flow and the subarachnoid spaces surrounding the brain and filled also with CSF [10]. The difficulties in modelling the system do not arise from the identification of these compartments but rather from their physical couplings, may it be direct (with matter transfer) through the Sylvius aqueduct or more subtle and indirect through the brain strains modulations (brain's volume variation under blood flow). It is clear that whatever the model, the mathematical representation of these couplings determines the nature of the model, abstract or intuitive. An abstract model, even if quantitatively relevant, might lead to severe difficulties in its handling and could not be useful in diagnosis assistance.

One of the most relevant approach is the handling of electrical analog [11]. It consists in associating with the intracranial system an equivalent electrical circuit. As was pointed out in the introduction, this way of modelling is usually ad hoc, that is the circuit is not derived from a biomechanical model built up from first principles. Nevertheless, it is clear that this approach assumes a linear dynamics of the intracranial system and profits by both the simplicity of the laws of electricity and an interesting intuitive ground. Even if the assumed linearity seems to be a reasonable assumption, it generally suffers a lack of justification. Nevertheless, it is always possible to introduce non-linearity in these circuits but their intuitive nature might be lost. Its complexity might be defined as the number of "parameters," that is the values of the constitutive elements of the circuit such as resistors, coils and capacitances it contains to which must be added the dimension of the associated vector-states space. The multiplication of the compartments (reflecting the structural complexity) and over all of the couplings between them leads to increasing "complexity" in the naïve sense we just gave.

The main interest of this approach relies on the simple computation of the transfer functions between different parts of the system (e.g., CSF and blood flow). Usually, the comparison to any available data allows for the determination of some of the parameters but for complex circuits, the residual parameters leads to an arbitrariness of the model which is not satisfactory. One of the main restrictions in the use of these ad hoc electrical analogues relies on the unfaithful correspondence between the parameters of the circuit (resistors, capacitances, etc.) and the biophysical parameters (objective parameters: viscoelasticity of the tissues, geometry of the system, etc.) of the system it "mirrors." But this restriction is not essential compared to their heuristic value, that is their predictive content and their ability to mimic some pathological situations of great interest for physicians.

Another way of describing the intracranial dynamics is incarnated in the so-called pressure-volume models [12]. A brief survey of these models is given in Appendix A. It should be noticed that the equations of these models, provided they are linear, have a direct interpretation in terms of electrical circuits. Nonlinearities are likely to occur for complex pressure-volume relationships (see, for example, Marmarou [13]). The most usual form of these linear models written for a set of compartments (number N) coupled to each other by fluid exchange reads

$$\forall i \in \{1,2,\ldots,N\} C_i \frac{dp_i}{dt} = -\sum_j \gamma_{ij}(p_i - p_j) + S_{iexc}. \quad (1)$$

The parameters C_i are the compliances of the compartments, $p_i(t)$ the pressure of the fluid within each compartment (these are the dynamical variables), γ_{ij} the conductances associated with the fluid exchange processes between the ith compartment and all the other ones indexed by j coupled to it and S_{iexc} is any time dependent external excitation such as cardiac pulses. In the linear approximation, the compliances are allowed to depend only on the stationary values of the pressure. As the conductance matrix $[\gamma_{ij}]$ is usually symmetrical and over all positive, the dynamical system described by (1) is expected to be stable. The notion of stability we refer to here is the structural stability (or instability) that is in keeping with the control parameters (compliances, conductances, etc.). Laplace or Fourier transforming the last equation makes it very easy to determine the amplitudes of the pressure variations within the compartments.

The construction of electrical analogues might be systematic if we associate to Eq. (1) a graph with a discrete function on the graph associating to each summit (the compartments)

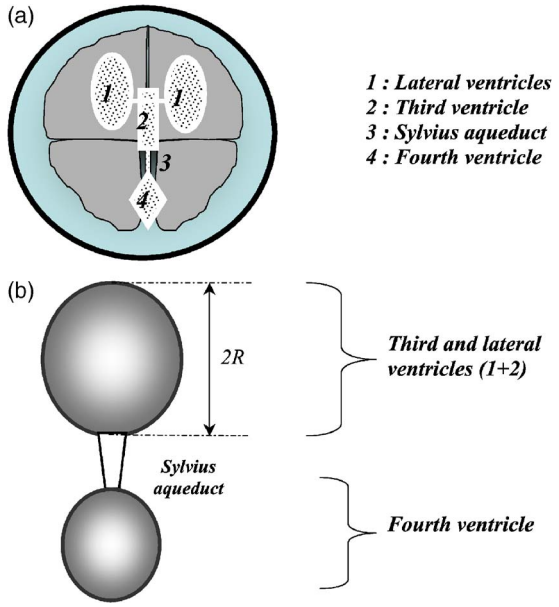

FIG. 1. (Color online) (a) Anatomical structure of the ventricular system composed of the two lateral ventricles connected with the third one separated from the fourth ventricle by the Sylvius aqueduct. (b) Simplification of the ventricular system to a spherical geometry. The lateral and third ventricles are "collapsed" into a unique sphere of radius R surrounded by the ependyma treated as an elastic membrane. That sphere is connected by the Sylvius aqueduct to the fourth ventricle.

a pressure p_i and a flow on that graph associating to each pair of summits a conductance γ_{ij}. Eq. (1) constrains severely the nature of the circuit: whatever the electrical interpretation of the graph, this circuit should be topologically equivalent [14] to that graph.

III. A MODEL FOR THE VENTRICLE DYNAMICS

A. Simplification of the anatomical structure of the ventricular system

The model dealt with in this paper is based on a simplification of the actual structure of the intracranial system. Indeed, the anatomy of the system, presented on Fig. 1(a) shows clearly a set of four interconnected ventricles. The paired lateral ventricles are connected through the foramina of Monro [15]. The third ventricle is connected to the fourth via the Sylvius aqueduct. This last ventricle allows a direct CSF flow into the subarachnoid spaces. The simplification consists in reducing the lateral ventricles and the third one to a unique spherical compartment with radius R delimited by an elastic membrane the ependyma as can be seen on Fig. 1(b). This choice of a spherical symmetry is in fact a first step towards a more realistic modeling of the ventricular system actually in progress. As this complex shape of the ventricular system arises from the inhomogeneous distribution of the stress field at its boundary, we expect that a deeper analysis will reveal the irrelevant nature of ventricles' geometry in their pathological behaviours. Nevertheless, this simplification of the ventricles geometry is often met in the literature [3,4] since it allows workable models of the ventricles deformation dynamics.

B. Fundamental equations of the model

The ependyma is treated as a very thin membrane endowed with known viscoelastic properties. We assume a steady state to exist for this ventricular compartment which is far from its equilibrium value. More precisely, the steady value of the radius $\bar{R}$ is bigger than its equilibrium value R_e in such a way that, in the absence of any excitation, the ventricle tends to collapse. This spontaneous trend is of course opposed by the CSF pressure. The existence of such a nonequilibrium steady state arises from the regulation processes within the intracranial system. Each ventricle is clearly an open system exchanging matter (CSF) with its exterior. The total CSF mass variation $dM/dt=\dot{M}$ reads then

$$\frac{1}{\rho}\dot{M} = \frac{dV}{dt} + V\frac{d}{dt}(\ln \rho) = I_S - I_a - \gamma(p - p_{ext}) \tag{2}$$

where $V(t)$ is the volume of the ventricles and $\rho(t)$ the CSF density at any time t, p and p_{ext} are respectively the average pressure in the abovementioned "spherical compartment" composed of the 3rd and lateral ventricles and in the 4th one, γ the hydrodynamical conductance of the aqueduct, I_S and I_a the volumic CSF secretion and resorption rate in the compartment. The time variation of the average density mirrored in the derivative $(d/dt)(\ln \rho)$ arises from the constant temperature compressibility $\chi_T \equiv (1/\rho)(\partial\rho/\partial p)_T$ of the CSF itself (which is rather negligible as shall be seen below). To account for the matter exchange processes and the displacement of the ependyma we will set

$$M(t) = M_e[1 + h(t)],$$

$$V(t) = V_e[1 + \varepsilon(t)], \tag{3}$$

where the index "e" refers to the equilibrium values of the parameters (mass, volum and density of the CSF). The function $h(t) \equiv (M - M_e)/M_e$ is an a-dimensional parameter which captures the global CSF mass variation due to exchange with other compartments and $\varepsilon(t) \equiv (V - V_e)/V_e$ the relative deformation of the ventricular area. Equation (2) then reads

$$V_e\left[\chi_T(1 + \varepsilon) + \left(\frac{\partial\varepsilon}{\partial p}\right)\right]\dot{p} = I_S - I_a - \gamma(p - p_{ext}). \tag{4}$$

A first interesting approximation of this nonlinear equation can be derived if we focuse on the dynamics of the pressure fluctuations around the stationary state $(\bar{p};\bar{R})$. It consists in replacing the second term into the square bracket $(\partial\varepsilon/\partial p) \times (p) \approx (d\varepsilon/dp)_{p=\bar{p}}$ leading us to the simplified model

$$V_e\left[\chi_T(1 + \bar{\varepsilon}) + \left(\frac{d\varepsilon}{dp}\right)_{p=\bar{p}}\right]\dot{p} \approx I_S - I_a - \gamma(p - p_{ext}). \tag{5}$$

The linearized scheme we are led to can be classified in the pressure-volume models category with an effective compli-

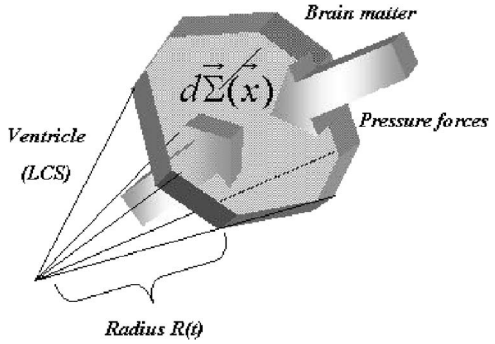

FIG. 2. This scheme sums up the notations we used in the description of the ependyma's motion. The infinitesimal piece of ependyma of area $d\Sigma(x)$ is centered about the point x. The displacement field is radial due to spherical symmetry and results from the action of the pressure forces of the brain matter and the CSF and the restoring force due to the elasticity of ependyma's tissues. In our model, we neglected the dissipative nature of the membrane dynamics.

ance associated with the ventricular compartment,

$$C(\bar{p}) = V_e\left[\chi_T(1+\bar{\varepsilon}) + \left(\frac{d\varepsilon}{dp}\right)_{\bar{p}}\right] = \bar{V}\left[\chi_T + \left(\frac{d\ln(1+\varepsilon)}{dp}\right)_{\bar{p}}\right]. \tag{6}$$

The derivative term in (6) might be considered as an effective contribution to the compressibility of the CSF which depends on the elastic properties of the ependyma and its vibrational dynamics. The nonlinear corrections to the model are very easy to derive from Eq. (5) by adding the higher order terms of the expansion of the right-hand side of (4). More precisely, if we get back to Eq. (5), the corrections to the linear scheme lead to a modulation of the effective compressibility of the CSF. In fact, the contribution of the derivative term is the dominating one since CSF is incompressible, that is $\chi_T \approx 0$. We will keep this reasonable assumption in our linear model. The effective compliance then reads

$$C(\bar{p}) \approx 4\pi\bar{R}^2\frac{d\bar{R}}{d\bar{p}} \tag{7}$$

which corresponds to the usual definition of the compliance.

The complete calculation of the steady compliance requires the adjunction to Eq. (5) of the motion equation of the elastic ependyma. As can be seen on Fig. 2, the ependyma is modeled as a thin membrane with thickness submitted to the action of pressure forces due to the CSF within the ventricles (pressure p_{in}), the stress field σ_b within brain matter and a restoring force arising from the elasticity of the membrane. The simplifying assumptions we made about the spherical symmetry of the ventricular space allows us to treat the stress σ_b as a pressure (p_{out}), that is the associated force due to the brain is normal to the ependyma. The high symmetry of the problem simplifies also the form of the displacement field $u(x,t)$ at any point x of the ependyma at any time t which appears to be radial that is

$$\vec{u}(\vec{x},t) = (R(t) - R_e)\vec{n}, \tag{8}$$

where $R(t)$ is the curvature radius of the spherical ependyma at time t, R_e the equilibrium value of that radius, and n the normal vector at point x. The complete motion equation of the ependyma and its solution are derived in Appendix B. The spectra of the variations of the relevant parameters such as $R(t)$ or the pressure $p(t)$ are dominated by low frequencies since our system is excited by cardiac pulses. This allows us, equivalently to neglect the effects of inertia and the viscous damping as can be clearly seen in Appendix B. It is thus clear that within this approximation the ependyma's displacement becomes

$$R(t) - R_e \approx \frac{(p_{in} - p_{out})}{\sigma k} \tag{9}$$

that is the pressure forces are opposed the restoring force depending on both the density of the ependyma through the parameter σ and its elastic constants through the parameter k. More precisely, as the ependyma is treated as a spherical elastic membrane (thickness l), our constant k depends on the Young modulus E of the ependyma and its Poisson modulus σ_p through the relationship [16],

$$k = 12\pi El/M(1-\sigma_p^2), \tag{10}$$

where M is the mass of the ependyma. It should be noticed that the parameter k has the units of a squared frequency. The pressure p_{in} in formula (9) is precisely the pressure at the surface of the ventricular CSF. It is related to the inner average pressure p through Laplace's law [17] $p - p_{in} = 2\Gamma/R$ where the constant Γ is the surface tension of the CSF that is the amount of energy to be provided to the confined CSF to increase its surface by one area unit. We are thus led to a very important additional relationship

$$p - p_{out} = \frac{2\Gamma}{R} + \sigma k(R - R_e). \tag{11}$$

It should be kept in mind that the range of validity of this law is intimately related to our assumption of a very slow dynamics of the system. It is then valid in the steady state. Equation (10) plays the role of a state equation relating the pressure within the compartment to its size. The formulas (6), (7), and (11) are the basic equations of our model. The last equation allows for the determination of the radius of the compartment knowing the pressure within. It also allows for the calculation of the compliance (7). This will be done in the next section devoted to the consequences of our model and to the assessment of some parameters.

IV. DYNAMICAL INSTABILITIES

A. Conditions for pressure regulation

The steady compliance in Eq. (7) then reads

$$C \approx 4\pi\bar{R}^2\frac{d\bar{R}}{d\bar{p}} = 4\pi\bar{R}^2\frac{1}{k\sigma - 2\Gamma/\bar{R}^2}. \tag{12}$$

This equation is derived from Eq. (11) where it is assumed that the pressure within the brain matter is constant and in-

dependant from the radius R. We regard this expression as the compliance of the system because it corresponds to the coefficient, endowed with the right units, of the pressure derivative term in the dynamical Eq. (5). According to Eq. (12), it exhibits an amazing algebraic nature arising from the compelling effects of the elastic properties of the ependyma and the surface tension of the ventricular CSF and will be referred to as the effective compliance of the system {ventricle delimited by the ependyma+CSF}. The definition of effective parameters is an intellectually comfortable point of view which allows for maintaining the usual meaning of the parameters and their intuitive content. If we had neglected the influence on the system of the CSF surface tension Γ, we would have been led to an always positive compliance $C_0 = 4\pi\bar{R}^2/\sigma k$ which can be thought off as that of the "empty" ventricular compartment. Rewriting Eq. (12) as a function of that last compliance, readily,

$$C = C_0 \Big/ \left(1 - \frac{2\Gamma}{\bar{R}^2 \sigma k}\right), \tag{13}$$

we are led to the idea that the empty compartment compliance C_0 is renormalized in the presence of CSF. As told previously, such a compliance usually thought to be positive, is in fact algebraic. As this delicate point could legitimately be considered as schocking by the experienced reader, we would like to highlight the significance of such an algebraic compliance and precise what should be meant by "effective compliance." It has in fact a dynamical sense in keeping with the structural instabilities (driven by the control parameters) its change of sign might induce. Indeed, the expression (13) shows that we can attribute a compliance C_0 (that is positive) to the ventricular compartment but alter the elasticity k of the ependyma which is "softened" by the surface tension of the CSF, that is endowed with an effective elasticity $k_{eff} = k - 2\Gamma/\sigma\bar{R}^2$ for any value of the radius. The instability coincides here with a negative value of the effective elasticity that is with the absence of an effective restoring force acting on the ependyma so that no stationary value of the radius of the ventricle does exist any more. The system loses then its ability to regulate the CSF pressure within. We can conclude that "pathological" behaviors of the dynamics are expected when the effective compliance becomes negative: it should remain positive for the intracranial system to be stable, that is for it to be able to regulate the pressure within the compartment under study.

The stability condition requires a minimum value of the ventricular compartment radius:

$$\bar{R} > \sqrt{\frac{2\Gamma}{k\sigma}}. \tag{14}$$

This minimal radius coincides with a minimal ventricular pressure value which prevents the ventricular compartment from collapsing. It is worth noticing that this minimal radius value does exist only because of a nonvanishing surface tension Γ of the CSF. In the vanishing Γ limit, that is when we neglect its influence on the system, the dynamics appears to be always stable, with no lower bound on the radius of the compartment. It is in striking opposition with the observation of a finite value of the average radius of the ventricles.

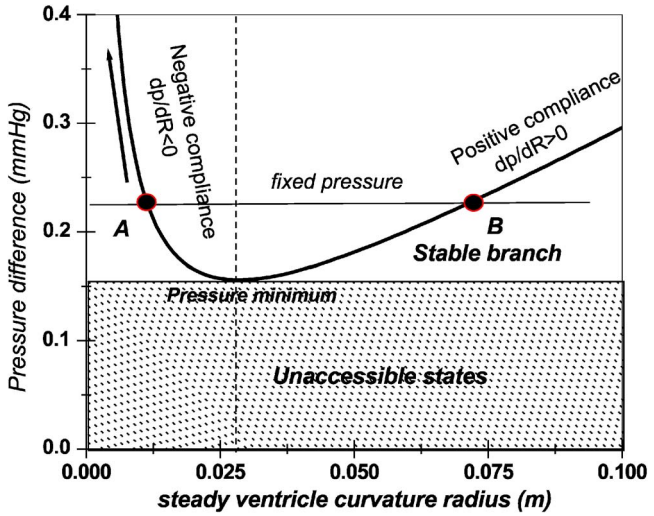

FIG. 3. (Color online) Plot of the pressure difference against the steady value of the radius of the ventricles. The existence of an unstable branch and a minimal pressure arises from a non-vanishing surface tension of the CSF. The minimal pressure corresponds to an infinite effective compliance (rigid limit). Below this pressure are lying states unaccessible to the system (shaded area).

For any given value of the radius, it is realised when the CSF surface tension is low enough or when the ependyma's elasticity is high enough. Indeed, introducing the ependyma's mass $M = \sigma 4\pi\bar{R}^2$, the last condition reads

$$k > 8\pi\Gamma/M(\equiv k_C). \tag{15}$$

There is thus a critical value of the elastic modulus k of the ependyma, or equivalently of the Young modulus E, below which the system is unstable. Physiopathologies of the ependyma's tissues might lead to an alteration of their mechanical properties and thus the ependyma's ability to regulate the volume (and the pressure within) of the ventricular space. The rupture of the ependyma is an extreme injury with the same consequences. Equation (15) might either be read in a different way. If an irreversible alteration of the elasticity of the tissues was to happen in such a way that (15) would not be valid, a decrease in the CSF surface tension Γ below a critical value $\Gamma_c = Mk/8\pi \propto 2El$ could restore the situation. According to our approach, the CSF surface tension and the ependyma's elasticity are the fundamental parameters controling the intracranial pressure regulation.

It is worth noticing that all these arguments suggest a strong correlation between these dynamical instabilities and some pathologies of the intracranial dynamics such as hydrocephalus. A simple mechanism arises then from the stability condition (14): it merely suggests that when the ventricle's radius is too small (below the minimal value required by the biophysical properties of the system), the system will spontaneously dilate until it reaches that value to recover its ability to regulate the intracranial pressure.

The main conclusion we drew about the stability of our system is illustrated on Fig. 3. We reported on this figure the

steady (differential) pressure given in Eq. (11) as a function of the ventricle's radius. It can be seen that each pressure value corresponds to two curvature radii, e.g., to the points *A* and *B*. The point *A* being located on the "unstable" branch that is to a negative compliance, is not realized contrary to the state labeled *B* located on the stable branch. If the system is released on state *A*, then any pressure fluctuation within the compartment is magnified exponentially due to its negative compliance as indicated by the black arrow on the figure. For the system to regulate the pressure around its fixed value, it has to move to the stable steady state B with radius increasing with the pressure as expected from the stability condition. At point B, the system is trapped by the pressure (and ventricle volume) regulation processes. It is clear that any point of the positive compliance branch corresponds to a stable steady state of the ventricular system. According to our view, a ventricle dilation process should occur after a slow steady pressure increase (due for instance to excessive CSF secretion). In that case, the dilation process might be viewed as a transition between steady states of the system.

We intend now to give some order of magnitude estimations. Taking for the CSF a surface tension close to water [18] at ambient temperature $\Gamma \approx 72.8 \times 10^{-3}$ N m^{-1} and a minimal value of the ventricle's radius $R_{\min} \approx 2$ cm [9] leads to a stability constraint $\sigma k > 3.6 \times 10^{-4}$ N cm^{-3}. If we double the minimal radius value, the last condition is less constraining since $(\sigma k)_{\min}$ is four times smaller. It is also possible from (10) to assess the compliance of the ventricle area. Indeed, retaining the typical value $E \approx 10^5$ Pa of the ependyma's Young modulus [4], a thickness ≈ 500 μm and a Poisson ratio $\sigma_p \approx 0.5$, we are led to the so-called empty compartment's compliance $C_0 \approx 0.25$ ml/mm Hg. This value agrees quite well with those encountered in the litterature [19].

B. Characteristic time in the structurally stable region

We aim here to give a further analysis of our dynamical model and show that it allows to compute explicitly the relaxation time of the ventricular compartment. Equation (5) provides a complete and realistic model for the intracranial system only when we incorporate the CSF resorption processes. The precise form of the resorption term I_a depends of course on the resorption mechanism [20]. Within the ventricular compartment, we will drop the contribution arising from the veinous absorption and retain only the transependyma diffusion. Its permeability to CSF is well known [21] but it is a dominant process only in extreme situations such as in some physiopathologies of the CSF flow (e.g., Sylvius aqueduct obstruction). As was told previously, the ependyma is a thin membrane of thickness separating two compartments—brain tissues and ventricles—allowing to maintain a radial pressure gradient $\Delta p/$ (see Fig. 4). The CSF flowing through that membrane reads then simply

$$I_a \approx 4\pi \bar{R}^2 D \frac{\Delta p}{l}, \qquad (15')$$

where $\Delta p = p - p_b$ is the pressure difference between the compartments and D is the diffusion coefficient proportional to

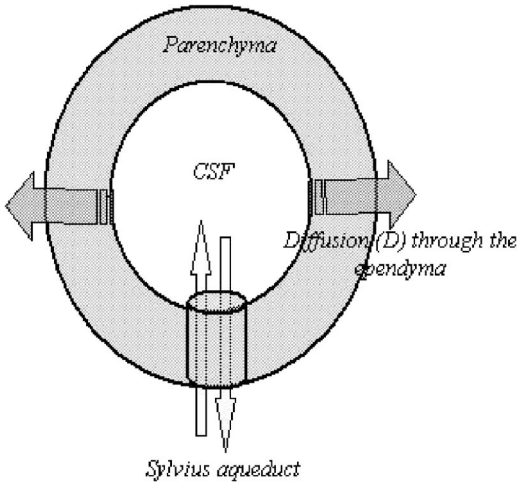

FIG. 4. Details of the CSF exchange between the third ventricle and the fourth ventricle. The direct coupling between these compartments holds through the Sylvius aqueduct. A lower amplitude flow holds through the ependyma which offers the CSF a permeability D or equivalently an effective conductance $\gamma_{ep} = 4\pi D \bar{R}^2 / l$.

the CSF permeability of the ependyma. The equation controlling the pressure fluctuations dynamics becomes

$$C(\bar{p})\dot{p} + \left(\gamma + D\frac{4\pi\bar{R}^2}{l}\right)p \approx I_S + \gamma p_{ext} + D\frac{4\pi\bar{R}^2}{l}p_b. \qquad (16)$$

The right-hand side describes the pressure within the fourth ventricle, in the brain and the secretion term as excitation terms. These terms are of course modulated at the cardiac frequency but a complete determination of these terms require to build up a complete model of the intracranial system taking into account the brain tissues dynamics and the coupling between the compartments. We are interested here only in the assessment of the characteristic time of the system. This time τ deduced from (16) reads

$$\frac{1}{\tau} = \frac{\gamma + 4\pi D\dfrac{\bar{R}^2}{l}}{C_{eff}}, \qquad (17)$$

where C_{eff} is the effective compliance given by formula (12). The last expression can be rewritten after a straightforward calculation $1/\tau = (1/\tau_0)\phi(X)$ where appears a characteristic time scale $\tau_0 = /lk\sigma D$ and the function ϕ fourth-order polynomial of the a-dimensional parameter $X = R_e/\bar{R}$ proportional to the curvature $1/\bar{R}$ of the ependyma, which reads

$$\phi(X) = 1 + \frac{l}{4\pi R_e^2 D}\left(\gamma - \frac{8\pi\Gamma D}{k\sigma l}\right)X^2 - \frac{\Gamma\gamma l}{2\pi R_e^4 D k\sigma}X^4 \equiv 1 + aX^2 - bX^4. \qquad (18)$$

The meaning of the constants a and b are made obvious by this expression. An order of magnitude estimation of the characteristic time scale is given by the product $R_h C_0$ [time constant of Eq. (16)] where $R_h (= 1/\gamma) \approx 75$

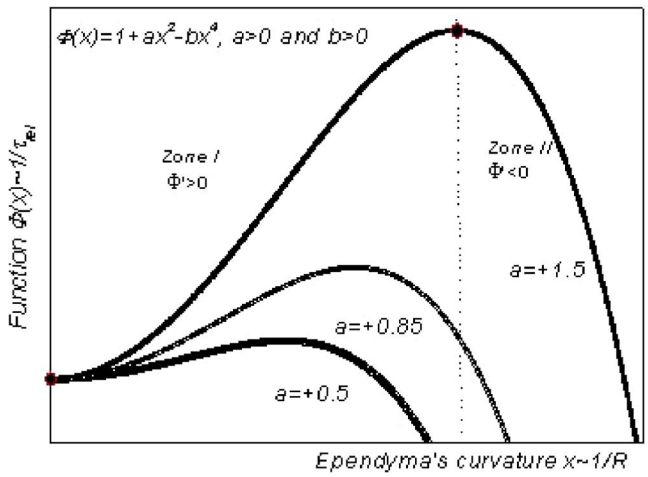

FIG. 5. (Color online) Plots of the function $\phi(X)$ proportional to the reciprocal relaxation time, against the ependyma's curvature for increasing values of the parameter $a>0$. Two regions denoted zone I and II are clearly distinguished, corresponding to $\phi'(X)$ positive or negative. In this case, the function exhibits two extremal values.

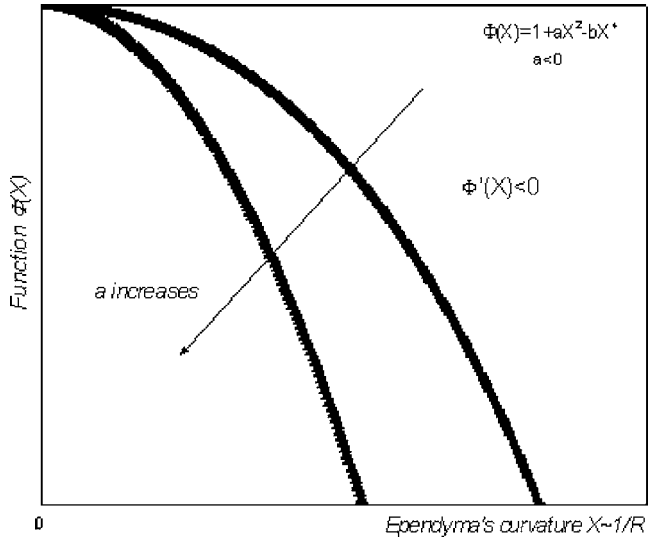

FIG. 6. Plots of the function $\phi(X)$ against the ependyma's curvature X for the parameter $a<0$. Only the region II remains and the associated relaxation time increases with the curvature. Its minimal value is realized for zero curvature.

$\times 10^{-6}$ mm Hg s/mm^3 is the hydrodynamical resistance of the Sylvius aqueduct with length $l \approx 20$ mm, a section $S_{aq} \approx 7$ mm^2 and the CSF viscosity $\eta_{CSF} \approx 10^{-3}$ Pa s. We are led to a typical time $\tau_0 \approx 2 \times 10^{-2}$ s which is much shorter than the heart beat period (1 second).

When the effective compliance is positive, that is in the structurally stable zone (see Fig. 3), the time τ should be considered as the relaxation time of the ventricular compartment, that is the time required for a complete resorption of any pressure fluctuation (around the steady value). It is interesting to notice that the polynomial (18), apart from the sign of the quartic term, looks like the so-called Landau potential (or even Higgs potential) usually met in the theory of second-order phase transitions [22] of condensed systems. By analogy, the coefficient of the quadratic term in (18) exhibits a critical value of the conductance of the Sylvius aqueduct $\gamma_C = 8\pi\Gamma D/k\sigma l$ and we subsequently expect two different dynamical behaviors when $\gamma < \gamma_c$ or $\gamma > \gamma_c$ suspected to hide pathological behaviors. Oppositely, as was pointed out previously, a vanishing CSF surface tension or the absence of any transpendymar diffusion process eliminates these regimes and leads to an obviously stable behavior. The plots of the function $\phi(X)$ for positive ($\gamma > \gamma_C$) and negative ($\gamma < \gamma_C$) parameter a are given in Figs. 5 and 6, respectively. As we restricted ourselves to the positive compliance region, we limited the plots to the range of positive curvatures for which the function $\phi(X)$ is positive. We divided the first plot into two regions characterized by the sign of the derivative $\phi'(X)$. These regions are characterized by two remarkable points, the minimum of $\phi(X)$ ($X=0$) and the maximum of $\phi(X)$ ($X^2 = a/2b = R_e^2 k\sigma(\gamma - \gamma_C)/4\gamma$ if $a>0$). When $a<0$, the state $X=0$ is turned into a maximum and the function $\phi(X)$ decreases monotonously. We will show in the next section the relevance of this subdivision in the analysis of the relaxational dynamics.

C. Relaxational dynamics

1. Pressure fluctuations damping

When $\phi(X)>0$, the characteristic time of our system for any steady value of the ependyma's curvature can be deduced form the causal Green function [23] of Eq. (15)

$$h(t;X) = \begin{cases} e^{-\phi(X)t/\tau_0}, & t>0 \\ 0 & \text{otherwise} \end{cases} \tag{19}$$

or equivalently from its Fourier transform,

$$H(\omega, X) = 1/\left(j\omega + \frac{1}{\tau_0}(1 + aX^2 - bX^4) \right) \tag{20}$$

This last expression is of high interest since it coincides with the transfer function between the ventricular pressure and the outer compartment pressure. It is clear from these expressions that the ventricular compartment might be viewed as a low-pass filter with a cutoff frequency $\omega_C \phi(X)$ depending on the steady curvature of the ependyma. If we neglect both the CSF surface tension ($\Gamma \to 0$) and the transependymar diffusion ($D \to 0$), the cutoff frequency reduces to $\omega_C \propto k\sigma\gamma/4\pi R_e^2$. It is then clear that for "normal" values of the conductance γ and the elasticity k, the cutoff frequency is high enough. Oppositely, in the case of an aqueduct's obstruction or any abnormal elastic behavior of the ependyma (low k and γ) the cutoff ω_C is vanishingly small corresponding to an infinite relaxation time: the ventricles lose their ability to regulate the pressure. In these limits, it is clear from Eq. (16) that the only nonvanishing term being the CSF secretion rate I_S, we expect a ventricle dilation. This point will be developped in the last section.

2. Stability towards fluctuations

The conclusions of the last section are valid only for a well defined curvature X. In fact, the relaxational dynamics

of the system, that is its ability to resorb any pressure fluctuation, is more complex. Indeed, the pressure p within the ventricles is always associated with some random fluctuations (noise) around its steady value. These pressure fluctuations induce random fluctuations $\delta X \equiv X - \bar{X}$ of the curvature obeying a stationary probability (density) distribution $p(\delta X)$. The efficiency of the regulation processes maintaining the system around its steady state might be measured by the variance $\sigma_X^2 = \langle \delta X^2 \rangle \equiv \int_{-\infty}^{+\infty} p(\delta X) \delta X^2 d(\delta X)$ which should be as small as possible. In the presence of fluctuations, the Green function (19) (or its Fourier transform) must be averaged over the fluctuations [22]

$$\langle h(t;X) \rangle = \int_{-\infty}^{+\infty} p(\delta X) e^{-(t/\tau_0)\phi(\bar{X}+\delta X)} d(\delta X) \overset{\text{F.T.}}{\leftrightarrow} \langle H(\omega) \rangle = \left\langle \frac{1}{j\omega + \phi(X)/\tau_0} \right\rangle. \tag{21}$$

The fluctuations thus lead to a broadening of the steady state of the system, turning the initial stability problem into the question of the stability towards fluctuations. The system's ability to regulate the pressure will depend on the existence of this average Green function [24] or equivalently of an effective relaxation time.

This necessary handling of the average Green function is justified by the stochastic nature of our dynamical equation in the presence of fluctuations (random coefficients). It has non trivial consequences on the dynamical behaviour of our system and thus on the electrical analogs to be built up (see the next section). Unluckily, the calculation of the average Green function is made difficult both by the unknown probability distribution of those fluctuations and the high order of the polynomial $\phi(X)$. Nevertheless, there are some workable limiting cases generating approximations relevant from both a physical and a clinical point of view. The simplest approximation consists in dropping the fourth order term in the function $\phi(X)$. This approximation is valid as far as $X \ll \sqrt{|a|/b}$ that is for high enough curvature radii. The average Green function reads then

$$\langle h(t;X) \rangle = e^{-(t/\tau_0)\phi(\bar{X})} \int_{-\infty}^{+\infty} p(\delta X) e^{-(t/\tau_0) a \delta X^2} e^{-(2t/\tau_0) a \bar{X} \delta X} d(\delta X), \tag{22}$$

where it is clear that a should be positive for the integral to exist whatever the probability distribution. Should it be otherwise, the system is unstable towards fluctuations. In the stable regime, that is $a > 0$, the precise form of this function is a very important factor since it determines the electrical analogs associated with our system. The distribution probability is the key parameter which seems difficult to extract from Eq. (22) with a simple procedure.

The modeling of the fluctuations probability density is the only way to assess the function (22). Thus, assuming a Gaussian probability distribution centered about the stationary curvature $\bar{X}$ with a width σ_X, Eq. (22) reads

$$\langle h(t;X) \rangle = \frac{h(t,\bar{X})}{\sqrt{2\pi}\sigma_X} \int_{-\infty}^{+\infty} e^{-(u^2/2)(1/\sigma_X^2 + 2a(t/\tau_0))} e^{-2a(t/\tau_0)\bar{X}u} du. \tag{23}$$

The detailed calculation reported in Appendix C leads to the final expression,

$$\langle h(t;X) \rangle = \frac{1}{\sigma_X} \left(\frac{\tau_0}{2at} \right)^{1/4} e^{-t/\tau_0} e^{-at\bar{X}^2/\tau_0(1+2a\sigma_X^2 t/\tau_0)} \tag{24}$$

whose long time behavior $t\tau_0/2a\sigma_X^2$ is not trivial

$$\langle h(t,X) \rangle \frac{1}{\sigma_X} e^{-\bar{X}^2/2\sigma_X^2} \frac{e^{-t/\tau_0}}{(2at/\tau_0)^{1/4}}. \tag{25}$$

The frequency dependence of its Fourier transform is then $\langle H(\omega) \rangle \propto 1/(j\omega + 1/\tau_0)^\beta = e^{-j\beta \arctan(\omega\tau_0)}/(\omega^2 + 1/\tau_0^2)^{\beta/2}$ where the power $\beta = 3/4$.

The main conclusions to be drawn from this section are that the system is stable towards fluctuations (regulation of the pressure fluctuations and well defined stationary state) only when $a > 0$ as was expected and that the presence of fluctuations gives rise to new non trivial dynamical regimes. Though difficult, it should be interesting to extract the exact fluctuation spectrum from the measurements of the Green function h since its interpretation restricts severely the possible electrical analogues.

3. Electrical analogues

The linearized dynamics of the ventricular pressure variations expressed in Eq. (16) suggests very simple electrical analogues. Indeed, if as usual we interpret the pressure within the coupled compartments as electrical potential and the flow I_S as a current, Eq. (16) can be rewritten as a simple current balance equation (nodes' law),

$$I_S = C\dot{p} + \gamma(p - p_{ext}) + \frac{D4\pi\bar{R}^2}{l}(p - p_b) \tag{26}$$

leading to a simple parallel RC circuit. A supplementary resistance can be added in parallel with the compliance C to model the dissipative properties of the ventricular dynamics we neglected in our model (low frequency dynamics). The coupling of the *SAS* (pressure p_{ext}) to the brain (pressure p_b) can be modeled by any additional circuit which is unknown but might be deduced from a modeling of the global intracranial dynamics. This circuit is of course very simple but there are many other ways to generate electrical analogues. For instance, the ventricular compartment could be regarded as a filter if the right-hand side of (16) is interpreted as an excitation (input) and the ventricular pressure as the response to that excitation (output). The filter is then as was pointed out in a previous section, a low-pass filter with a transfer function given by (19). These electrical analogues are simple and intuitive since their components involve only the relevant physical parameters $(D, \gamma, \ldots)$. They allow for modeling both the normal (healthy) situation corresponding to high γ values (or $a > 0$) and pathological ones such as a severe obstruction of the aqueduct associated with the vanishing γ limit.

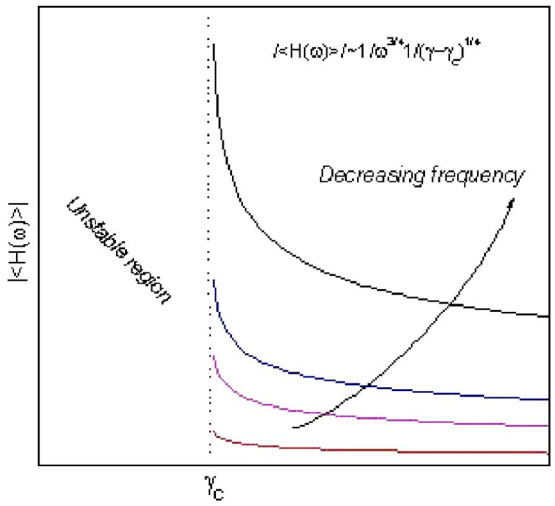

FIG. 7. (Color online) Plots of the magnitude of the transfer function against the conductance of the Sylvius aqueduct at different arbitrary frequencies. When approaching the "critical" conductance, this magnitude diverges with a critical exponent 0.25. This behavior indicates the vicinity of an unstable region.

There is no evidence in such an approach for any instability since all the coefficients are positive. As was shown previously in our physical model, instability towards random pressure fluctuations are evidenced in a stochastic model. But the electrical analogues to be associated with the stochastic model are not trivial. This is made clear by the Fourier transform of Eq. (25), which at high enough frequency reads

$$\langle H(\omega)\rangle \approx \frac{\tau_0}{\sigma_X}\frac{1}{(2a_0(\gamma-\gamma_C))^{1/4}}e^{-\bar{X}^2/2\sigma_X^2}\frac{1}{(j\omega\tau_0)^{3/4}}\ (\gamma>\gamma_C). \tag{27}$$

This result clearly suggests the use of a nonintuitive electrical circuit (empirical) referred to as a constant phase element (CPE) [25] associated with an admittance $Y(\omega)\propto 1/(j\omega\tau)^{\alpha}$ where the exponent α is usually lying between 0.5 and 1 (in our case $\alpha=3/4$). In many situations of condensed matter physics where it is encountered, it has many causes. In our model, it originates from the randomness affecting the curvature (Gaussian fluctuation spectrum) or equivalently from the statistical distribution of relaxation times. The variation of the amplitude $|\langle H(\omega)\rangle|$ with the conductance γ at various frequencies is reported on Fig. 7. The unstable region is visible below the critical conductance γ_C. In the vicinity of the critical conductance (critical point), the transfer function strongly diverges (signature of the instability).

The main problem with these CPE-based models is the ill-defined capacitance to be associated with the system. Indeed, according to (27) a frequency-dependent capacitance seems unavoidable except if we consider restricted frequency ranges where the capacitance exhibits constant values likely to depend on these ranges. The problem is made more acute when remembering that this capacitance extracted from the electrical analogue is usually thought of as an assessment of the compliance of the compartment under study. This circumstance illustrates the limitation of any intuitive interpretation of the analogues which might generate any spurious values of the main parameters of the system. Thus, unlike the purely deterministic case modeling of the ventricles' dynamics by CPE seems more relevant since it accounts for any structural instability (pressure regulation instability) in keeping with specific pathologies of the intracranial dynamics. Nevertheless, the introduction of these non intuitive circuits doesn't allow for a direct assessment of the compliance.

V. RELATIONS TO HYDROCEPHALUS

In this section, we aim at discussing the possible applications of our model to hydrocephalus [9]. Hydrocephalus corresponds to the clinical effects accompanying the ventricles' distension [26]. A physical approach is rather "poor" to give a complete description of hydrocephalus: the clinical effects involve physiological processes whose complexity is out of the range of physics. We will thus focuse on the dilation process. In our model, dynamical instabilities are clearly identified which correspond to a lack of the intracranial pressure regulation. The sudden and uncontrolled pressure increase might lead to the ventricles' expansion.

A. Kinetic model of the dilation process

A description of the dilation process lacks. It should be postulated independently of our model. This description requires a kinetic equation ruling the time evolution of the curvature radius of the ependyma. An empirical law regarding slow dilation is known from the studies carried out by Milhorat [21] on a population of chimpanzees. The radius expands in two steps according to nearly linear laws,

$$R(t) \approx R_0 + \dot{R}_0 t \tag{28}$$

with a dilation rate $\dot{R}_0$ much smaller in the second step. The typical values of these rates were about 10% of the total radius per hour in the first step (lasting 6 hours) and 0.5% per hour during the second step (lasting 40 hours). Considering the case of an obstructive ($\gamma\to 0$) hydrocephalus and neglecting the transependymar flow ($D\to 0$), the ventricular pressure $\bar{p}(t)$ averaged over a cardiac cycle (we thus drop the modulated component) evolves according to the law

$$C(t)\frac{d\bar{p}(t)}{dt} \approx I_S, \tag{29}$$

where we defined a slowly varying compliance $C(t)4\pi R^2(t)/\sigma k$. The last equation then reads

$$C(0)\dot{\bar{p}}=I_S/(1+2t\dot{R}_0/R_0) \tag{30}$$

leading to a slow logarithmic variation of the pressure $\bar{p}(t)=[I_S t_0/C(0)]\ln(1+t/t_0)$, where we set $t_0=R_0/2\dot{R}_0$ and $C(0)$ is the initial compliance. This evolution is reported on Fig. 8 for different arbitrary values of the time scale t_0. These curves strongly resemble those reported by Milhorat with a slope at the origin $I_S/C(0)$. According to Milhorat's data

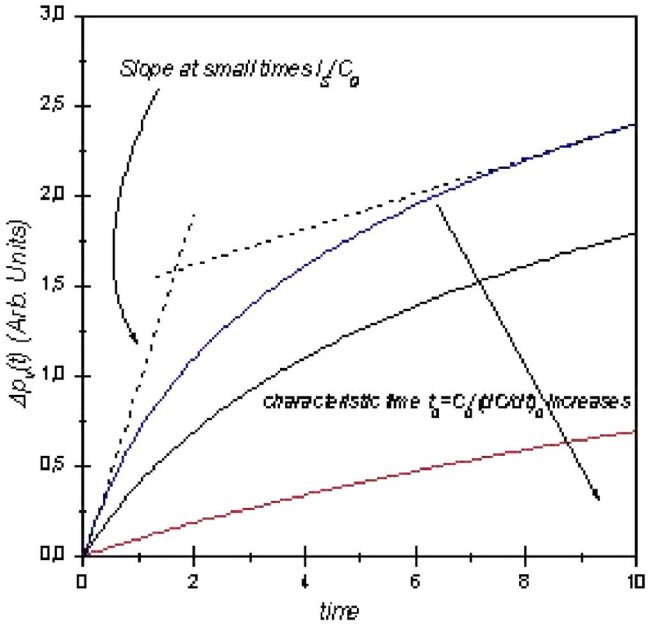

FIG. 8. (Color online) Obstruction of the aqueduct leads in our model to a logarithmic (slow) variation of the ventricular pressure. This prediction is in good agreement with the data reported by Milhorat [21]. Two different regimes can be distinguished at short and long times with a slowing down at long times.

$\dot{R}_0/R_0 \approx 0.1\ \mathrm{h}^{-1}$ leading to a typical time $t_0 \approx 5$ h and the initial pressure variation rate $\dot{p}_0 20(\mathrm{ml/h})/0.25(\mathrm{ml/mm\ Hg}) = 80\ \mathrm{mm\ Hg/h}$.

B. Spontaneous dilation in the non stationary regime

We can get a step further by evaluating the way the Green function (19) is modified in the presence of a dilation. When the curvature depends slightly on time $\bar{X}=\bar{X}(t)$, this function reads

$$h(t,\bar{X}(t)) = e^{-\int_0^t \phi(\bar{X}(t'))(dt'/\tau_0)}. \tag{31}$$

Taking into account the slow variations of the curvature, we obtain the expansion $\int_0^t \phi(\bar{X}(t'))dt' \approx t\phi(\bar{X}(0)) + t^2/2[\partial\phi(\bar{X})/\partial\bar{X}\cdot\dot{\bar{X}}(t)]_0 + \cdots$ truncated to second order. The response function finally reads

$$h(t,\bar{X}(t))e^{-t\phi(\bar{X}_0)/\tau_0}e^{-(t^2/2\tau_0)(\partial\phi/\partial\bar{X})_{\bar{X}(0)}\dot{\bar{X}_0}} \equiv e^{-\alpha t}e^{-\beta t^2/2}, \tag{32}$$

where the index zero attached to the curvature and related magnitudes indicate initial values and the constants α and β are short notations easy to deduce form (32). From (32) we deduce that in the nonstationary regime (curvature kinetics), the stability condition (finite Green function) reads $\beta = (1/\tau_0)\dot{\bar{X}}_0(\partial\phi/\partial\bar{X})_0 > 0$. Two situations are then possible. For $a>0$, if the system is dropped in a state located in the first zone of Fig. 5 ($\phi'>0$), we expect $\dot{X}>0(\dot{R}<0)$ that is the system contracts spontaneously. If dropped in the zone II ($\phi'<0$), we expect oppositely $\dot{X}<0$, that is the system undergoes a spontaneous dilation. Finally, at the point realizing the maximum value of the function ϕ, that is the shorter relaxation time, the system should be oscillating (stable point). For $a<0$ (e.g., obstruction of the Sylvius aqueduct), the system is offered only one possibility: spontaneous dilation till the minimal value ($X=0$) of the relaxation time is realized (in fact it is never reached). We are thus led to the following interesting conclusion: Spontaneous dilation of the ventricles occurs for unstable systems to minimize their relaxation time. Moreover, the pathological situations should be identified with the case $a<0$ for which no stationary state exists. For highlighting the strong correlation of this last regime with hydrocephalus, it is worth noticing that the instability condition should be read in many ways if written as

$$\gamma k\sigma/D < 8\pi\Gamma/l. \tag{33}$$

It is clear that it might be realized in different ways leading to a naive classification scheme of pathologies. Abnormally small values of the aqueduct's conductance γ correspond to obstruction (in the physiological sense), total obstruction corresponding to a vanishing γ. Abnormal elastic behavior of the ependyma corresponds to small values of the modulus k. In that case, a normal CSF transfer through the aqueduct is present but the unability of the system to regulate the intracranial pressure arises from a too low restoring force of the ependyma. The last case corresponds to abnormally high values of the diffusion constant D, that is to an abnormally high value of the ependyma's permeability to CSF. A high CSF flow through the parenchyma (acting as a poroelastic medium) is then expected. In that case the mass transfer between the subarachnoid space and the ventricular system is dominated by this transependymar diffusion. This flow is not totally balanced by the direct transfer through the aqueduct (too low) and a kind of "closed loop" flow is expected. Further calculations to understand quantitavely this unsteady regime are necessary (this requires a modeling of the parenchyma structure) but it seems in keeping with the so-called normal pressure hydrocephalus [9]. These last consequences suggest a possible unified physical description of hydrocephalus.

We would like to conclude this section by computing the transfer function associated with these pathological situations. A straightforward Fourier transform of (32) leads to

$$H(\omega) = e^{-j\omega\alpha/|\beta|}e^{-\omega^2/\omega_C^2}. \tag{34}$$

It corresponds to the transfer function of a Gaussian low-pass filter with a cutoff frequency $\omega_C = \sqrt{2|\dot{X}_0(\partial\phi/\partial X)_0|}/\tau_0 = \sqrt{2|\dot{X}_0|a_0X_0|\gamma-\gamma_c|}$. The cutoff frequency thus scales as $\omega_C \propto (\gamma_c-\gamma)^{1/2}$. A large cutoff should correspond to a fast dilation and a small one to a very slow dilation.

VI. CONCLUSION

To address the problem of ventricles' dilation as a possible instability of the intracranial dynamics, we built up from first principles a model focusing on the third and lateral ventricles' compartment excited by its coupling to the fourth one (CSF exchange through the Sylvius aqueduct endowed with an appropriate hydrodynamical conductance) and to

brain matter. The third and lateral ventricles were treated as a unique spherical compartment of CSF delimited by the ependyma treated as an elastic closed membrane. The obtained dynamical equation is linearized around a steady state characterized by an effective algebraic compliance depending on both the geometry of the compartment, the ependyma's elasticity and the CSF surface tension.

This model bears some instabilities of different nature characterized by a lack of the ventricular pressure regulation. The first one is a structural instability revealed by the change of sign of the effective compliance which occurs for a CSF surface tension lower than a critical value proportional to the ependyma's Young modulus and its thickness. In the positive effective compliance region, we were able to compute the relaxation time of the system identified as a Landau like fourth order polynomial of the ependyma's curvature. As in the Landau theory of phase transitions, the instability is driven by the quadratic term a proportional to $(\gamma - \gamma_C)$ where γ is the Sylvius aqueduct's conductance. Two different regimes of the relaxational dynamics are predicted according to the sign of a. The difference in these regimes is evidenced through the response of the system to random pressure fluctuations, that is the behavior of the causal Green function of the dynamical equations averaged over the fluctuations distribution. We have shown that for $a > 0$, the transfer function is that of a non trivial low-pass filter identical to a *constant phase element* suggesting interpretation of the dynamics in terms of nonintuitive circuits. Oppositely when a is negative, the system is shown to be unstable towards a spontaneous dilation of the ventricle which acts as a gaussian low-pass filter whose cutoff frequency scales as $(\gamma_C - \gamma)^{1/2}$. Finally, using a simple model for the dilation kinetics inspired by the data obtained by Milhorat in a population of chimpanzees, we have established a clear correlation between this last instability and hydrocephalus.

Further studies, and especially a systematic comparison of our model to MRI data obtained on a human population (to assess the main parameters of our model), are in progress to validate this possible interpretation of hydrocephalus as intracranial dynamics' instabilities.

APPENDIX A

In this appendix we aim to give further details regarding the models of the intracranial dynamics of the type pressure-volume usually referred to in the literature. These models rely on the CSF mass conservation law and the mechanisms of secretion and absorption of CSF. The balance mass equation reads,

$$dV/dt = (\textit{CSF formation rate}) - (\textit{CSF absorption rate}) = I_S - I_a, \tag{A1}$$

where $V(t)$ is the CSF total volume at any time t within the studied compartment, and the terms I_S and I_a are respectively the CSF secretion and resorption rate, that is the CSF volume created or absorbed per unit time. We would like to emphasize, as was pointed out in the body of the text, that this equation governs the long-term dynamics of the CSF volume. More precisely, it doesn't take into account the modulation of the CSF due to cardiac pulses (short time or fast dynamics) since the CSF secretion/absorption process is characterized by a characteristic time longer (a few hours) than the cardiac pulses period (a second). It is obtained very simply by averaging over several cardiac cycles (this procedure averages out the cardiac modulation of the density and velocity of the CSF) and integrating over the whole compartment volume the continuity equation,

$$\mathrm{div}(\rho v) + \frac{\partial \rho}{\partial t} = \bar{\rho}(I_S - I_a), \tag{A2}$$

where ρ is the CSF density at any time ($\bar{\rho}$ its average constant density) and the velocity field ν captures the pulsatile nature of the CSF flow generated by cardiac pulses. The secretion and absorption rates act of course as sources term. This is a local equation characterizing the fluid flow. Its implication on the global dynamics of the system fluid +compartment frontier will depend on the boundary conditions imposed to our system. For instance, as is usually the case, if the compartment is limited by an elastic membrane (such as the ependyma), the global dynamics might be derived from integrating Eq. (A2) throughout the mobile frontier of the compartment. It thus generates extra terms due to the elastic deformation of the frontier contributing the time variation of the pressure within the compartment. A systematic implementation of this procedure is very difficult because the lack of knowledge of the dynamical laws governing the elastic deformations or the complex geometry of the membrane. Many authors circumvent these difficulties by retaining in these elastic deformations the only associated variations of the volume of the compartment and introduce an ad hoc parameter, the so-called compliance C of the fluid compartment. The parameter C is a measurement of the storage capacity in volume determined by the elastic (or viscoelastic) properties of the system. The global dynamics of the pressure, assumed to be first order (if inertia is neglected) reads then,

$$C(P)\frac{dP}{dt} + \frac{P}{R_a} = I_f(t) + \frac{P_e}{R_a} + S(t), \tag{A3}$$

where $C(P)$ is the pressure-dependent compliance, P the pressure within the compartment, R_a is any "hydrodynamic" resistance corresponding to a fluid exchange with any other compartment with a pressure P_e (this might be of course a blood vessel), I_f is the source term and $S(t)$ any excitation term (e.g., blood pulsatile flow). Equation (A3) represents an infinity of models since there are many ways to choose the analytical dependence of the compliance with pressure. A strictly linear model corresponds to a constant compliance. But non linear model were also produced by Marmarou [13] or Sklar [12]. Whatever the precise dependence on pressure chosen for the compliance, the main problem is unsolved: there is no systematic method to compute this compliance which would allow for a deeper understanding of it and its eventual role in the intracranial dynamics pathologies.

APPENDIX B

In this appendix we aim at deriving the ependyma's motion equation and its solution relating the time evolution of its radius $R(t)$ to the average pressure $p(t)$ within the ventricles. The motion equation of an infinitesimal piece of ependyma (see Fig. 2) endowed with a mass $\delta m=\sigma d\Sigma$ (or superficial mass σ) then reads,

$$\delta m\ddot{R} = -\eta\delta m\dot{R} - k\delta m(R-R_e) + (p_{in}-p_{out})d\Sigma, \quad \text{(B1)}$$

where k is the elastic constant of the ependyma and η is the viscous damping coefficient. This equation which is trivially projected onto the normal direction to the ependyma is the simplest model we can build up. According to this oversimplified view, the ependyma might be viewed as a spring with constant k and damping coefficient η. Fourier transforming this equation leads to the simple solution expressed as a convolution

$$R(t) = R_e + \frac{1}{\sigma}\int_{-\infty}^{+\infty} h(t-t')[p_{in}(t')-p_{out}(t')]dt', \quad \text{(B2)}$$

where $h(t')$ is the causal Green function of Eq. (B1),

$$h(t') = \int_{-\infty}^{+\infty} \frac{1}{-\omega^2+k+i\omega\eta} e^{i\omega t'} d\omega \ \text{if} \ t'>0 \ \text{and 0 otherwise.} \quad \text{(B3)}$$

It is then clear that the Fourier spectra of the pressures (and the ventricular radius) involved in all these equations are dominated by low frequencies because of the cardiac excitation, that is their amplitudes are negligible when the frequencies are high enough. According to Eq. (B2), the ventricle's radius spectrum is dominated by low frequencies. Subsequently, we can restrict ourselves in (B3) to the low frequency range ($\omega \ll \sqrt{k}$). Indeed, the Green function can be expanded as

$$h(t') \approx \frac{1}{k}\delta(t') - \int_{-\infty}^{+\infty} \frac{i\omega\eta-\omega^2}{k} e^{i\omega t'} d\omega + \int_{-\infty}^{+\infty} \left(\frac{i\omega\eta-\omega^2}{k}\right)^2 e^{i\omega t'} d\omega + \cdots. \quad \text{(B4)}$$

Substituting this expansion in (B2) and taking into account the restriction of the pressure spectrum to low frequencies, we can drop all the terms of the expansion but the first one. Within this approximation, Eq. (B2) becomes

$$R(t) - R_e \approx \frac{p_{in}(t)-p_{out}(t)}{\sigma k}. \quad \text{(B5)}$$

APPENDIX C

In this appendix we calculate the expression obtained in (23). This equation can be rewritten

$$\langle h(t,X)\rangle = h(t,\bar{X})\frac{\Psi(u)}{\sqrt{2\pi}\Gamma}, \quad \text{(C1)}$$

where we set $u=(2at/\tau_0)\bar{X}$ and introduced the function $\Psi(u)=\int_0^{+\infty} e^{-x^2/2\Gamma^2} ch(ux)dx$ depending on the parameter $1/\Gamma^2=1/{\sigma_X}^2+2at/\tau_0$. An integration by parts leads to the new expression

$$\Psi(u) = \frac{1}{u\Gamma^2}\int_0^{+\infty} xsh(ux)e^{-x^2/2\Gamma^2}dx = \frac{1}{u\Gamma^2}\frac{\partial\Psi}{\partial u}. \quad \text{(C2)}$$

We then have to solve a first order differential equation with an initial condition $\Psi(0)=\sqrt{2\pi}\Gamma$. Its solution reads

$$\Psi(u) = \sqrt{2\pi}\sigma_X e^{(u^2/2)\Gamma^2} = \sqrt{2\pi}\frac{1}{(1/{\sigma_X}^2+2at/\tau_0)^{1/4}} \exp\left(2a^2\frac{t^2}{\tau_0^2}\bar{X}^2\frac{{\sigma_X}^2}{1+2a{\sigma_X}^2\frac{t}{\tau_0}}\right), \quad \text{(C3)}$$

$$\langle h(t,X)\rangle = \frac{1}{(1/{\sigma_X}^2+2at/\tau_0)^{1/4}}\frac{1}{\sigma_X}e^{-t/\tau_0} \times\exp\left(2a^2\frac{t^2}{{\tau^2}_0}\bar{X}^2\frac{{\sigma_X}^2}{1+2a{\sigma_X}^2\frac{t}{\tau_0}} - at\bar{X}^2/\tau_0\right) = \frac{1}{(1/{\sigma_X}^2+2at/\tau_0)^{1/4}}\frac{1}{\sigma_X}e^{-t/\tau_0} \times\exp\left(-a\frac{t}{\tau_0}\bar{X}^2\frac{1}{1+2a{\sigma_X}^2t/\tau_0}\right), \quad \text{(C4)}$$

from which follows the long time behavior obtained in Eq. (25).

[1] F. Magendie, J. Physiol. Exp. Pathol. **4**, 399 (1824).
[2] J. O'Connell, Brain **66**, 204 (1943).
[3] R. Bloch and A. Talalla, J. Neurol. Sci. **27**, 485 (1976).
[4] M. Kaczmarek, R. P. Subramanian, and S. R. Neff, Bull. Math. Biol. **59**, 295 (1997).
[5] G. Tenti, J. M. Drake, and S. Sivaloganathan, Neurol. Res. **22**, 19 (2000).
[6] O. Baledent, M. C. Henry-Feugeas, and I. Idy-Peretti, Invest. Radiol. **36**, 368 (2001); O. Baledent *et al.*, Invest. Radiol. **39**, 45 (2004).
[7] N. Alperin *et al.*, M.R.I. Magn Reson Med. **35**, 741 (1996).
[8] *Hydrocephalus*, edited by K. Shapiro, A. Marmarou, and H. Portnoy (Raven Press, New York, 1984).
[9] S. Hakim, J. G. Venegas, and J. D. Burton, Surg. Neurol. **5**, 187 (1976).
[10] H. Rouvière and A. Delmas, *Anatomie humaine, descriptive,*

topographique, fonctionnelle (Masson, Paris, 2002), Vol. 1.
[11] G. Kongolo, O. Balédent, K. Ambarki, R. Bouzerar, and M. E. Meyer, International Interdisciplinary Workshop on Flow and Motion, Zurich, 2004.
[12] F. H. Sklar and I. Elashvili, J. Neurosurg. **47**, 670 (1977); S. Sivaloganathan, G. Tenti, and J. M. Drake, Appl. Math. Comput. **94**, 243 (1998).
[13] A. Marmarou, K. Shulman, and R. M. Rosende, J. Neurosurg. **48**, 332 (1978).
[14] A. Sache, *Théorie des graphes*, coll. Que sais-je? (Presses Universitaires de France, Paris, 1974); O. Ore, *Theory of Graphs* (AMS, Providence, 1962), p. 38; I. U. Thoma *Introduction to Bond Graphs and Their Applications* (Pergamon, New York, 1975).
[15] G. Lazorthes, *Le Liquide Céphalo Rachidien*, 3rd ed. (Masson, Paris, 1983).
[16] L. Landau and E. Lifchitz, *Théorie de l'élasticité*, Phys. Théorique Vol. 7 (MIR, Moscow, 1967).
[17] L. Landau and E. Lifchitz, *Mécanique des fluides*, Phys. Théorique Vol. 6 (MIR, Moscow, 1971).
[18] V. N. Kazakov, A. F. Vozianov, O. V. Sinyachenko, D. V. Trukhin, V. I. Kovalchuck, and U. Pison, Adv. Colloid Interface Sci. **86**, 1 (2000).
[19] S. Sorek, J. Bear, and Z. Karni, Ann. Biomed. Eng. **17**, 1 (1989); see also Ref. 4.
[20] H. Davson, F. R. Domer, and J. R. Hollingsworth, Brain **96**, 329 (1973).
[21] T. H. Milhorat, M. K. Hammock, and P. P. Mc Grath, Arch. Neurol. **22**, 397 (1970); D. Levine, Bull. Math. Biol. **61**, 875 (1999).
[22] J. C. Toledano and P. Toledano, *Landau Theory of Phase Transitions* (World Scientific, Singapore, 1987); C. Kittel, *Introduction à la Physique de l'état solide*, 7ème édition (Dunod, Paris, 1998).
[23] M. Braun, *Differential Equations and their Applications: An Introduction to Applied Mathematics*, 3rd ed. (Springer-Verlag, New York, Berlin, 1986).
[24] G. Adomian, Rev. Mod. Phys. **35**, 185 (1963).
[25] J. R. MacDonald, *Impedance Spectroscopy* (John Wiley, New York, 1987).
[26] A. Pena *et al.*, Acta Neurochir. Suppl. (Wien) **81**, 59 (2002).